

# ANALYSIS OF ULTRA-FAST KELVIN WAVES SIMULATED BY KYUSHU UNIVERSITY GCM

JP4.4

Ying-Wen Chen\* and Saburo Miyahara  
Kyushu University, Fukuoka, JAPAN

## 1. INTRODUCTION

Equatorial Kelvin waves are one of prominent global scale wave motions in the equatorial region. This kind of waves only propagates toward east and its structure is trapped in the equatorial region. Matsuno (1966) theoretically found that equatorial Kelvin waves exist in the equatorial region. The structure of equatorial Kelvin waves is symmetric about the equator and there is only zonal wind but no meridional wind exists. The relation between the pressure and the wind fields is that westerlies dominate in the high-pressure region while easterlies dominate in the low-pressure region.

Various observations have found that Kelvin waves exist in the atmosphere and shown that this kind of waves is one of prominent global scale motions and prominent periods of Kelvin waves vary with height in the equatorial region. Wallace and Kousky (1968) indicated using balloon observations that Kelvin waves are primarily with zonal wavenumber 1 and 2 ( $S=1$  and 2) and in the period range of 10-20 days in the lower stratosphere. Hirota (1977) showed that  $S=1$  type Kelvin waves with periods about 10 days in the upper stratosphere and lower mesosphere by rocket observations. By satellite observations, Salby (1983) showed that equatorial Kelvin waves in the period band of 3-6 days with  $S=1$  in the lower mesosphere. Kelvin waves in the period band of 3-6 days are called ultra-fast Kelvin waves. Ultra-fast Kelvin waves were also found in the mesosphere and lower thermosphere region by radar observations (Riggin et al., 1997;

Pancheva et al., 2004). In the paper, Pancheva et al. (2004) especially indicated that the vertical wavelength of the zonal wind field of 3-day ultra-fast Kelvin waves in the lower thermosphere is about 49 km, which is consistent with numerical results shown by Forbes (2000).

In this study, we focus on the behavior of ultra-fast Kelvin waves in the Kyushu University General Circulation Model (the Kyushu-GCM). Behaviors of ultra-fast Kelvin waves in the Kyushu-GCM are investigated using methods of composite analysis, space-time Fourier analysis and E-P flux analysis. We also focus on the comparison between the theoretical solution for ultra-fast Kelvin waves and analyzed results.

## 2. DATA

The dataset used in this study is calculated by the Kyushu-GCM T42L250 version. This dataset includes the zonal wind, meridional wind, vertical wind, temperature, and geopotential height fields. The vertical coverage of this model is from the surface to height 150 km height with 250 layers. The vertical resolution in the stratosphere, mesosphere, and lower thermosphere is about 500 m. The horizontal resolution of this model is triangular-truncation at wavenumber 42. Physical processes that are thought to be excitation sources of equatorial waves such as moist convective heating (Forbes, 2000; Mayr et al., 2004) are included in this model. In this study, the bi-hourly sampled dataset of wintertime including December, January, and February, is used.

## 3. ANALYSIS METHODS

### 3.1 COMPOSITE ANALYSIS

We apply a band pass filter and Fourier

---

\*Corresponding author address: Ying-Wen Chen, Kyushu Univ., Dept. of Earth and Planetary Sciences, Fukuoka, Japan, 812-8581; e-mail: [yingwen@geo.kyushu-u.ac.jp](mailto:yingwen@geo.kyushu-u.ac.jp)

analysis on this dataset to extract out 2-3 days period with S=1. We apply composite analysis along these about 3-day period eastward propagating components to clarify the wave structure of these components. We apply composite analysis along eastward propagating phase line of about 3-day period to clarify the wave structure of these components.

### 3.2 SPACE-TIME FOURIER ANALYSIS

We use a space-time Fourier analysis method to separate eastward and westward propagating S=1 components of each field. For a space-time dependent function  $f(x, t)$ , it can be rewritten as follows:

$$f(x, t) = \sum_k \sum_{\omega} \{ W.C. \times \cos(kx + \omega t) + W.S. \times \sin(kx + \omega t) + E.C. \times \cos(kx - \omega t) + E.S. \times \sin(kx - \omega t) \}$$

where coefficients of westward cosine, westward sine, eastward cosine, and eastward sine coefficients are written as W.C., W.S., E.C., and E.S., respectively, and  $k$  denotes zonal wavenumbers, while  $\omega$  denotes periods.

## 4. ANALYSIS RESULTS

### 4.1 COMPOSITE ANALYSIS RESULTS

Figure 4.1.a shows the time-longitude section of 2- to 3-day period components of the geopotential height field of January where the latitude is 2.1°N and height is 100 km. As shown in this figure, the 2- to 3-day period components propagate toward east with time and is seen that the 2- to 3-day period components are mainly dominated by S=1 components. It is also found that wave amplitudes are comparatively strong in the duration from 15<sup>th</sup> January to 30<sup>th</sup> January. Similar behaviors are also found in the zonal wind field (not shown). We extracted out S=1 phase lines of the zonal wind, meridional wind,

and geopotential height fields of 2- to 3-day components and apply composite analysis along the about 3-day eastward propagating components of these three fields from 15<sup>th</sup> January to 30<sup>th</sup> January.

The horizontal structure of composite results at 100 km height is shown in figure 4.1.b. As shown in this figure, the structure of this wave is symmetric about the equator and the relation of winds and geopotential height fields has the structure of Kelvin waves. The maximum of the wind field appears at near the equator with about 20 ms<sup>-1</sup> and that of the geopotential height field also appears at the equator with 150 m. Similar results can also be found in the height region between 80 km and 120 km. Structures of Kelvin waves in the regions higher than 120 km and lower than 80 km become obscure and the meridional wind gets stronger.

Vertical sections of the zonal wind and geopotential height fields of composite analysis results at 2.1°N are shown in figure 4.1.c and 4.1.d. These two figures show phases of this wave tilt toward east with increasing height. This means that the energy propagation is upward while the phase propagation is downward. It also can be estimated from figures 4.1.c and 4.1.d that the vertical wavelength of this wave is about 40 km. This result is consistent with the theoretical vertical wavelength 52 km, which can be found by solving the Laplace's tidal equation, for 256 K isothermal atmosphere. This analysis result is also consistent with the observational result, which is found by Phancheva et al. (2004), showing that the vertical wavelength of the 3-day wave is about 49 km.

Figure 4.1.e shows the vertical profile of the amplitude of the geopotential height field averaged over 10.5°N to 10.5°S. As shown in this figure, the amplitude of the geopotential field grows at a rate of nearly  $\exp(z/2H)$  in the height region between 20 km and 100 km. This fact shows that this wave propagate vertically with nearly energy conserving in the height region between 20-100 km and this wave may be excited in the region below 20 km.

The energy propagating direction of this wave is shown in figure 4.1.f. This figure shows directions of the E-P flux of the 3-day composite analysis result. As shown in this figure, this wave almost propagates upward in the region higher than 40 km, which is consistent with the vertical sections shown in figures 4.1.c and 4.1.d.

## 4.2 SPACE-TIME FOURIER ANALYSIS RESULTS

Figure 4.2.a shows the period-height distribution of the eastward propagating with  $S=1$  of the zonal wind field at  $2.1^\circ\text{N}$  from the surface to 130 km. As shown in this figure, there is a peak appearing at period of 3-day for the wintertime three months. In this subsection, we focus on the wave structure of the 3-day period with  $S=1$  components for the wintertime three months.

The horizontal section of the wind, which includes the zonal wind and meridional wind fields, and geopotential height fields at 100 km is shown in figure 4.2.b. As shown in this figure, the wind and geopotential height fields satisfy the relation of the Kelvin waves. It also can be found in figure 4.2.b that the maximum of the wind field appears at near the equator is about  $10 \text{ ms}^{-1}$  and that of the geopotential height field also appears at the equator with 60 m. Similar results also can be found in the height region of 80-120 km (not shown). In the regions out of 80-120 km, the meridional wind gets stronger and structures of the Kelvin waves become obscure than that in the region of 80-120 km. Note that the maxima of results of space-time Fourier analysis are smaller than that of results of band pass filters, because the results of the space-time Fourier analysis shows the average condition of the winter time but not the duration that wave amplitudes are strong.

Vertical sections averaged over  $10.5^\circ\text{N}$  to  $10.5^\circ\text{S}$  of the zonal wind and geopotential height fields are shown in figures 4.2.c and 4.2.d. As shown in these two figures, phase lines of both the zonal wind and the geopotential height fields tilt toward east with increasing height. This shows that the energy

propagation of this wave is upward and the phase propagation is downward. It also can be estimated from these two figures that the vertical wavelength of this Kelvin wave is about 50 km. This result is consistent with the solution of the Laplace's tidal equation, which shows that the vertical wavelength is 52 km for 256 K isothermal atmosphere. The analyzed result is also consistent with the observation result shown by Phancheva et al. (2004), which showed that the vertical wavelength of 3-day waves is about 49 km.

Figure 4.2.e shows the vertical profile of the amplitude of the geopotential height field averaged over  $10.5^\circ\text{N}$  to  $10.5^\circ\text{S}$ . As shown in this figure, the amplitude grows at a rate of nearly  $\exp(z/2H)$ , which shows that this Kelvin wave propagates vertically with nearly energy conserving in the region between 20 km and 100km.

Figure 4.2.f shows the energy propagating direction of this Kelvin wave from the surface to 130 km shown by the direction of E-P flux. As shown in this figure, energy is propagating upward in the height region above 40 km, which is consistent with the results shown in figures 4.2.c and 4.2.d.

## 5. SUMMARY

The results of composite analysis and space-time Fourier analysis show that structures of the 3-day period Kelvin wave in the height region of 80-120 km can be clearly identified in the Kyushu-GCM. Phase lines of 3-day period Kelvin waves tilt toward east with increasing height shows that phases propagate downward and energy propagates upward. These results also show that the vertical wavelengths of the 3-day Kelvin wave of both composite analysis results and space-time Fourier analysis results are consistent with the theoretical solution, which can be obtained by solving the Laplace's tidal equation. By the E-P flux analysis (only directions are shown), it can be found that energy of the 3-day Kelvin wave propagates upward which is consistent with results shown in the vertical sections of the zonal wind and geopotential height fields. From the vertical

profile of the amplitude, it can be found that 3-day period Kelvin waves propagate upward under almost energy conserving condition from about 20 km to reach the mesosphere and lower thermosphere region.

## 6. ACKNOWLEDGEMENTS

Figures in this manuscript are produced by GFD-DENNOU Library (DCL).

## 7. REFERENCES

1. Andrews, D. G., J. R. Holton, and C. B. Leovy, 1987: Middle Atmospheric Dynamics (International Geophysics Series), P.150-217.
2. Forbes, J. M., 2000: Wave coupling between the lower and upper atmosphere: case study of an ultra-fast Kelvin Wave. *Journal of ATMOSPHERIC AND SOLAR-TERRESTRIAL PHYSICS*, Vol. 62, p.1603-1621.
3. Hirota, I., 1977: Equatorial Waves in the Upper Stratosphere and mesosphere in Relation to the Semiannual Oscillation of the Zonal Wind. *Journal of the Atmospheric Sciences*, Vol. 35, p.714-722.
4. Matsuno, T., 1966: Quasi-Geostrophic Motions in the Equatorial Area. *Journal of the Meteorological Society of Japan*, Vol. 44, p.25-43.
5. Mayr, H. G., J.G. Mengel, E. R. Talaat, H.S. Porter, and K. L. Chan, 2004: Modeling study of mesospheric planetary waves: genesis and characteristics. *Annales Geophysicae*, Vol. 22, p.1885-1902.
6. Riggins, D. M., D. C. Fritts, T. Tsuda, T. Nakamura, and R. A. Vincent, 1997: Radar observations of a 3-day Kelvin wave in the equatorial mesosphere. *Journal of Geophysical Research*, Vol. 102, No. D22, P.26, 141-26, 157.
7. Salby, M. L., D. L. Hartmann, P. L. Bailey, and J. C. Gille, 1983: Evidence for Equatorial Kelvin Modes in Nimbus-7 LIMS. *Journal of the Atmospheric Sciences*, Vol. 41, p.220-235.
8. Wallace, J. M., and V. E. Kousky, 1968: Observational evidence of Kelvin waves in the tropical stratosphere. *Journal of the Atmospheric Science*, Vol. 25, p.900-907.
9. Yoshikawa, M. and S. Miyahara, 2005: Excitations of nonmigrating diurnal tides in the mesosphere and lower thermosphere simulated by the Kyushu-GCM. *Advances in Space Research*, Vol. 35, p.1918-1924.

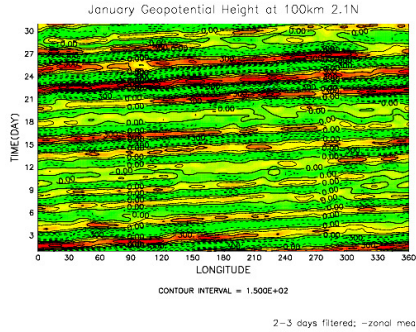


Figure 4.1.a: The time-longitude diagram of the 2- to 3-day period components of the geopotential height field of the January at 100 km.

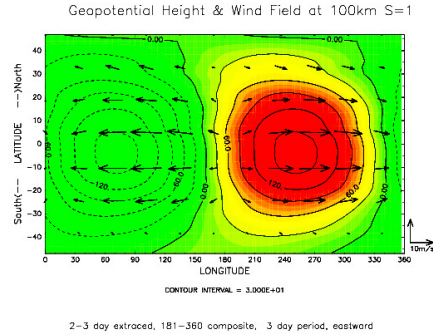


Figure 4.1.b: The horizontal section of the wind (arrows) and geopotential height (contours) at 100 km.

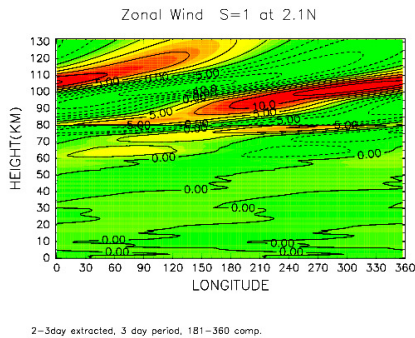


Figure 4.1.c: The vertical section of the zonal wind field at 2.1°N. Heights are from the surface to 130 km.

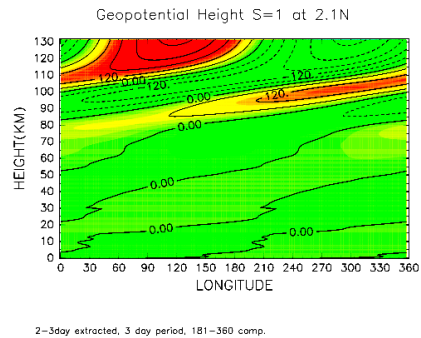


Figure 4.1.d: The vertical section of the geopotential height field at 2.1°N. Heights are from the surface to 130 km.

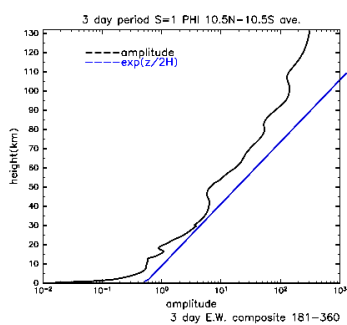


Figure 4.1.e: The vertical profile of the geopotential height field averaged over 10.5°N to 10.5°S. Heights are from surface to 130 km.

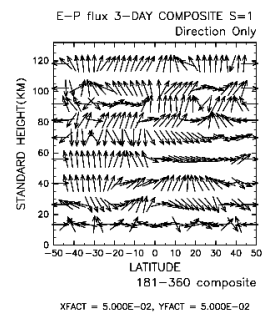
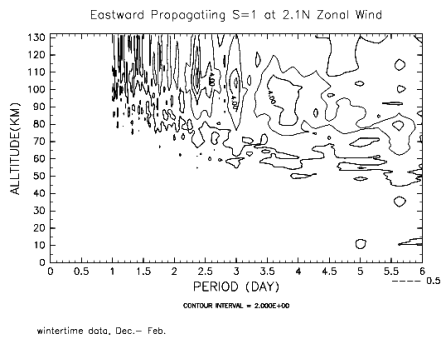


Figure 4.1.f: The directions of the energy propagation. Heights are from surface to 130 km.



wintertime data, Dec.- Feb.

Figure 4.2.a: The period-height distribution of the eastward propagating components of the zonal wind field. Heights are from surface to 130 km and periods are from 0-day to 6-day.

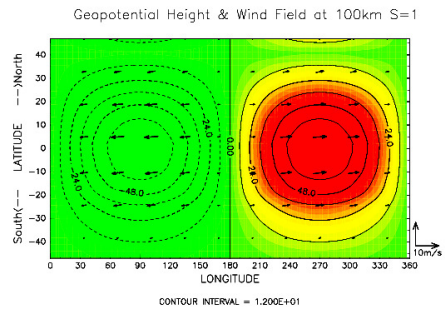
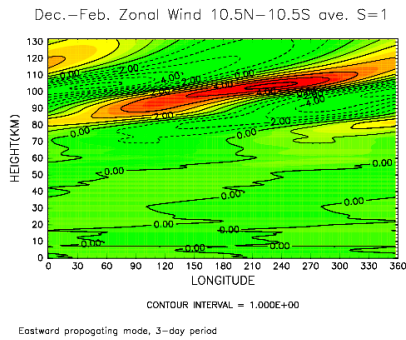
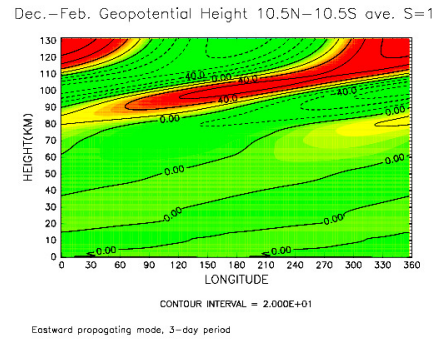


Figure 4.2.b: The horizontal section of the wind (arrows) and geopotential height (contours) at 100 km.



Eastward propagating mode, 3-day period

Figure 4.1.c: The vertical section of the zonal wind field averaged over 10.5°N to 10.5°S. Heights are from the surface to 130 km.



Eastward propagating mode, 3-day period

Figure 4.1.d: The vertical section of the geopotential height field averaged over 10.5°N to 10.5°S. Heights are from the surface to 130 km.

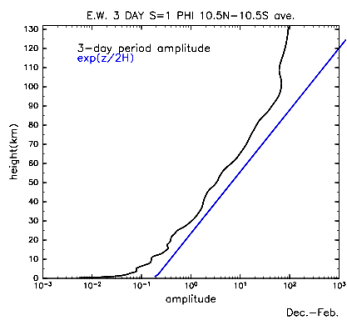


Figure 4.2.e: The vertical profile of the geopotential height field averaged over 10.5°N to 10.5°S. Heights are from the surface to 130 km.

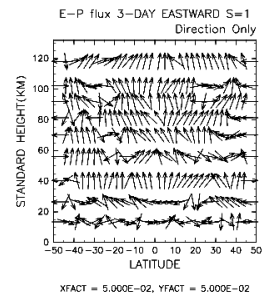


Figure 4.2.f: The directions of the energy propagation. Heights are from surface to 130 km.